MAMMOTHITE: A Pb-Sb-Cu-Al OXY-HYDROXIDE-SULFATE — HYDROGEN ATOM DETERMINATION LOWERS SPACE GROUP SYMMETRY

Joel D. GRICE[§]

Canadian Museum of Nature, PO Box 3443, Stn D, Ottawa, ON, K1P 6P4, Canada

Mark A. COOPER

Department of Geological Sciences, University of Manitoba, 125 Dysart Road, Winnipeg, MB, R3T 2N2, Canada

Abstract

The crystal structure of mammothite, $Pb_6Cu_4AlSbO_2(SO_4)_2Cl_4(OH)_{16}$, is monoclinic in acentric space group $C2$, with a 18.959(4), b 7.3398(19), c 11.363(3) Å, β 112.428(9)°, V 1461.6(1.0) Å^3, and $Z = 2$. It has been refined to an R index of 0.019 on the basis of 3878 observed reflections. There are three crystallographically distinct Pb sites with two different co-ordinations: $[Pb1O_8Cl_1]$ is a mono-capped square antiprism polyhedron, while $[Pb21O_7Cl_2]$ and $[Pb22O_7Cl_2]$ are tri-capped trigonal prisms. Both Cu^{2+} sites have distorted $[4 + 2]$ octahedral coordination due to the Jahn-Teller effect. The Al and Sb sites are regular-octahedral co-ordination with oxygen atoms. The $[SO_4]$ tetrahedron is quite distorted, with S–O bond lengths varying from 1.45 to 1.52 Å and subtended O–S–O angles varying from 106 to 113°. In the structure there are eight $(OH)^-$ anions. All eight H atoms *pfu* were located, and it is these structure sites that reduce the symmetry from centric to acentric. Although mammothite is classified as a framework structure, it has a distinct layering. There are two layer types in the mammothite structure that parallel (001). There are three octahedrally coordinated sites; two are occupied by Cu atoms and one by an Al atom, in the octahedral layer. The tetragonal dipyramids $[CuØ_6]$ are linked forming 'olivine-like' chains parallel to the **b**-axis. The second layer, termed the cross-linked layer, has three $[PbØ_9]$ polyhedra with shared edges forming chains parallel to the **b**-axis, like the $[CuØ_6]$ tetragonal dipyramids. These chains are cross-linked by edge-sharing $[SbO_6]$ octahedra and decorated with $[SO_4]$ groups. The H atoms are in 'holes' within both layers.

Keywords: mammothite, crystal structure, acentric, hydrogen atoms.

Introduction

Mammothite is a rare oxy-hydroxide-sulfate mineral with an exotic list of essential cations: Pb^{2+}, Cu^{2+}, Al^{3+}, and Sb^{5+}. Peacor *et al.* (1985) gave a complete description of the new mineral from the type locality in the Mammoth vein, Tiger, Arizona, USA and from the slags of Laurium, Greece. Effenberger (1985) used the Tiger, Arizona material to solve the crystal structure. With the technology of the time Effenberger was not able to locate the H atoms. In the present, using technology with more intense X-ray beams and more sensitive detectors, we are able to use much smaller crystals, reducing the effects of absorption that a mineral with this chemical composition has. Determination of the H atom positions established proof that the symmetry of mammothite is acentric $C2$ and not the centrosymmetric space group $C2/m$ that describes the structure of

the heavier atoms. Effenberger suspected this and alludes to this in her structure description of 30 years ago, but without the hydrogen positions the lower space group could not be proven.

The Rowley mine, Arizona is a third locality for the mineral and it is mentioned on web sites but no publication exists. The crystals are of good quality and provided an opportunity to refine the structure. The only difference between the original material and that of Rowley is a minor amount of additional Cr.

Geological Setting and Occurrence

Rowley mine, Theba, Painted Rock District, Painted Rock Mountains, Maricopa County, Arizona is a former Cu-Pb-Au-Ag-Mo-V-baryte-fluorite mine approximately 27 miles west and north of Gila Bend. Mineralization is the Rowley vein; a NE–SW striking

§ *Corresponding author e-mail address*: jgrice@mus-nature.ca

shear zone which may represent a fault with Tertiary andesite and rhyolite rocks to the NW and Precambrian schist to the SE (Stewart & Pfister 1960, Kirkemo *et al.* 1965). The Rowley vein actually comprises two veins within the same fault zone; a quartz vein in the foot wall and a baryte vein in the hanging wall. The Rowley mine is particularly well known for superb wulfenite specimens.

Material Studied

The sample with the mammothite crystals is largely baryte with minor vanadinite. The blue-green crystals of mammothite, up to 5 mm in size, are striated. A crystal was checked with an electron microprobe. The Cr_2O_3 values were variable up to a maximum of 0.3 wt.% Cr_2O_3. There was no Fe, Mn, Ti, V, Co, or Ni, so it is most likely the Cr content which is responsible for the green hue. Normally mammothite has a cobalt blue (cerulean blue) color.

X-Ray Crystallography

Crystal-Structure Determination

A single crystal of mammothite used for the collection of X-ray intensity data was a sliver measuring $40 \times 5 \times 4$ μm^3. Intensity data were collected using a fully automated Bruker D8 three circle diffractometer equipped with a rotating anode generator operating at 50 kV, 24 mA, with Mo$K\alpha$ radiation, multi-layer optics, and an APEX-II CCD detector. This setup yields a very intense X-ray beam and a significantly decreased lower detection limit. A full sphere of intensity data was collected up to $2\theta = 60°$ using 14 s frames at frame widths of $0.2°$ giving a total of 28,681 reflections (8573 within the Ewald sphere). Information relevant to the data collection and structure determination is given in Table 1. The three-dimensional data was corrected for Lorentz, polarization, and background effects, and an empirical absorption-correction was applied (SADABS, Sheldrick 1998), which reduced the

internal residual for merging data from 7.83% before the absorption correction to 4.50% after the absorption correction (for certain reflections). All calculations were done with the Siemens SHELXTL 5.1 system of programs (Sheldrick 1997), with scattering factors of neutral atoms taken from the International Tables for X-ray Crystallography (Ibers & Hamilton 1974). Assigning phases to a set of normalized structure-factors gave a mean value $|E^2 − 1|$ of 0.946, which suggests the centrosymmetric space-group $C2/m$.

For easy comparison the starting model for the refinement kept the site assignments and labels of Effenberger (1985). The structure was initially refined in centric $C2/m$ to $R = 0.0180$ for 2141 $Fo > 4\sigma(Fo)$ and 0.0207 for all 2307 data and including H positions that were not found in the Effenberger (1985) structure. In $C2/m$, the Oh1 and Oh2 anions are located on the mirror plane; the associated H positions (also lying on the mirror plane) gave refined isotropic displacement parameters that were much greater than those for the other H atoms in the structure, suggesting that the H atoms associated with the Oh1 and Oh2 anions would be better modeled off the mirror plane. These H atoms could be disordered across the mirror, with an equal likelihood of appearing on either side of the mirror, or they potentially could have an ordered arrangement in a lower symmetry model. We tested for this by refining in the space group $C1$, and discovered that the H positions in question were consistent with a lower symmetry ordered arrangement, and were able to establish the correct space group as $C2$. In order to facilitate comparison between our $C2$ model and the $C2/m$ model of Effenberger (1985), we constrained the Sb atom to $y = 0$. Additional sites generated by lowering the symmetry are labeled with the addition of a second digit. H positions determined from difference-Fourier maps were refined with soft constraints; O–H distance of 0.98 ± 0.02 and an isotropic displacement parameter was refined such that H positions related by a pseudo-symmetry i are correlated as equivalent. Note

TABLE 1. MAMMOTHITE: DATA COLLECTION AND STRUCTURE REFINEMENT INFORMATION

Space Group	$C2$ (SG # 5)	Measured reflections	8573
a (Å)	18.959(4)	Unique reflections	4302
b (Å)	7.3398(19)	Observed reflections [> $4\sigma(F)$]	3878
c (Å)	11.363(3)	R(merge)	0.0163
α (°)	90	Goodness of fit on F^2	1.05
β (°)	112.428(9)	R_1 index (%) for all data	2.37
γ (°)	90	R_1 index (%) for observed data	1.94
V (Å^3)	1461.6(1.0)	wR_2 (%) for all data	4.35
		Flack parameter	0.17(6)

Ideal unit-cell contents: $Pb_{12}Cu_8Al_2Sb_2O_4(SO_4)_4Cl_8(OH)_{32}$ μ = 38.9 mm^{-1}.
Refinement by full-matrix least squares on F^2.

TABLE 2. MAMMOTHITE ATOMIC COORDINATES AND ANISOTROPIC DISPLACEMENT FACTORS (Å²)

Site	x	y	z	U_{11}	U_{22}	U_{33}	U_{23}	U_{13}	U_{12}	U_{iso}	BVS[2]
Pb1	0.21039(1)	−0.00017(6)	0.17920(1)	0.01421(2)	0.01813(3)	0.01466(2)	0.0002(1)	0.00601(2)	0.0001(1)	0.01552(2)	2.120
Pb21	0.42314(1)	0.25876(1)	0.20361(1)	0.01857(4)	0.01230(4)	0.01957(4)	−0.00001(3)	0.00751(3)	−0.00248(3)	0.01675(3)	2.033
Pb22	−0.42306(1)	−0.25884(2)	−0.20331(1)	0.01872(4)	0.01216(5)	0.02217(4)	−0.00004(3)	0.00795(3)	−0.00199(4)	0.01764(3)	2.043
Cu1	0.24986(6)	0.2501(2)	0.5002(1)	0.01490(8)	0.0151(1)	0.01439(9)	−0.00306(7)	0.00417(7)	−0.00479(8)	0.01523(6)	1.907
Cu2	0.10434(1)	0.0001(1)	0.36849(2)	0.01237(8)	0.0129(1)	0.01601(8)	0.0014(4)	0.00763(6)	0.0008(4)	0.01309(5)	2.076
Al1[1]	0	−0.0005(4)	½	0.0094(2)	0.0121(3)	0.0088(2)	0	0.0032(2)	0	0.0102(2)	2.737
Sb	0	0	½	0.00907(5)	0.01262(7)	0.00989(6)	0	0.00346(4)	0	0.01058(4)	5.430
S	0.24971(2)	−0.0003(2)	−0.09612(4)	0.0106(2)	0.0124(2)	0.0118(2)	0.0009(6)	0.0041(1)	0.0006(6)	0.0117(1)	6.034
Cl1	0.36676(3)	0.0001(3)	0.39660(5)	0.0301(2)	0.0274(3)	0.0237(2)	−0.0003(8)	−0.0006(2)	0.0004(9)	0.0303(2)	0.837
Cl2	0.44955(3)	0.0004(2)	−0.19868(5)	0.0234(2)	0.0128(2)	0.0264(2)	−0.0018(7)	0.0099(2)	−0.0008(7)	0.0207(1)	1.229
O	0.00284(7)	0.0014(6)	−0.1708(1)	0.0126(6)	0.0158(6)	0.0078(4)	0.008(1)	0.0040(4)	0.0002(1)	0.0120(3)	2.203
Oh1[3]	0.23729(8)	0.0011(7)	−0.4412(1)	0.0232(6)	0.0154(6)	0.0154(6)	−0.002(2)	0.0027(5)	0.005(2)	0.0194(4)	1.881
Oh2	0.08877(7)	0.0012(7)	−0.3460(1)	0.0099(4)	0.0178(6)	0.0141(5)	0.003(2)	0.0046(4)	−0.001(1)	0.0140(3)	2.286
Oh31	0.08250(9)	0.1837(3)	0.0441(2)	0.0091(6)	0.024(1)	0.02127(8)	−0.0032(7)	0.0071(6)	−0.0005(7)	0.0178(5)	2.139
Oh32	−0.0839(1)	−0.1834(2)	−0.0423(2)	0.0180(7)	0.0051(7)	0.0181(7)	−0.0061(6)	0.0106(6)	−0.0072(6)	0.0126(5)	2.118
Oh41	0.0408(1)	0.1752(3)	0.4167(2)	0.0184(7)	0.0166(8)	0.0153(7)	−0.0009(6)	0.0115(5)	−0.0013(7)	0.0153(4)	2.244
Oh42	−0.0388(1)	−0.1722(3)	−0.4153(2)	0.0127(7)	0.0079(8)	0.0159(8)	−0.0032(6)	0.0027(6)	−0.0018(6)	0.0130(5)	2.192
Oh51	0.17048(9)	0.1838(3)	0.3401(2)	0.0112(6)	0.0117(8)	0.0124(7)	0.0021(6)	0.0017(5)	0.0006(6)	0.0126(4)	2.162
Oh52	−0.1708(1)	−0.1824(3)	−0.3403(2)	0.0166(8)	0.0125(8)	0.0146(8)	0.0000(7)	0.0042(6)	−0.0025(7)	0.0150(5)	2.170
Os1	0.17665(7)	0.0009(7)	−0.0716(1)	0.0120(5)	0.0349(8)	0.0160(5)	−0.007(2)	0.0067(4)	−0.001(2)	0.0206(4)	2.230
Os2	0.31345(8)	0.0015(8)	0.0268(1)	0.0164(6)	0.0309(8)	0.0206(6)	−0.002(2)	0.0005(5)	−0.005(2)	0.0246(4)	1.996
Os31	0.2467(1)	0.1632(3)	−0.1732(2)	0.031(1)	0.018(1)	0.032(1)	0.0080(8)	0.0061(8)	−0.0068(8)	0.0289(6)	2.251
Os32	−0.2495(1)	−0.1598(4)	0.1708(2)	0.037(1)	0.032(1)	0.024(1)	0.0156(9)	0.0025(9)	−0.012(1)	0.0340(7)	2.372
H1	0.237(1)	−0.056(2)	−0.364(1)							0.06(1)	1.195
H2	0.1343(5)	0.056(3)	−0.348(2)							0.09(2)	1.279
H31	0.072(1)	0.302(1)	0.071(2)							0.032(6)	1.209
H32	−0.0680(8)	−0.259(2)	−0.097(1)							0.032(6)	1.152
H41	0.0591(5)	0.264(1)	0.484(1)							0.042(7)	1.205
H42	−0.073(1)	−0.262(1)	−0.469(2)							0.042(7)	1.131
H51	0.1326(7)	0.279(2)	0.302(3)							0.033(8)	1.245
H52	−0.163(2)	−0.296(1)	−0.294(2)							0.033(8)	1.165

[1] refined site occupancy factor: Al 0.740(2) and Cr 0.260.
[2] bond valence parameters calculated using the constant of Malcherek & Schlüter (2007) for the H-Cl bond and Brese & O'Keeffe (1991) for all others.
[3] Oh denotes (OH)− anion.
[4] Os denotes oxygen atoms bonded in the sulphate group.

that H1 and H2 have drifted significantly off of the *m* plane that existed in *C2/m*.

The maximum and minimum electron-densities in the final cycle of refinement were +2.94 and –1.20 e⁻/Å³. Both the maximum and minimum electron-densities are close to Pb atoms. With all atoms located and assigning anisotropic displacement factors the structure refined in *C2* to *R* = 0.0195 for 3878 *F*o > 4σ(*F*o) and 0.0237 for all 4302 data. The slight increase in *R* value over that attained in space group *C2/m* (*R* = 0.0180) is due to a decrease in the number of observed reflections per least squares parameters refined. The increase is not statistically meaningful. The refining Flack parameter result of 0.17(6) reliably confirms that the correct absolute structural configuration was refined in the polar space group *C2*.

The final positional and anisotropic displacement parameters of atoms are given in Table 2 and selected bond-lengths and angles in Table 3. Table 4 details the hydrogen bonding in mammothite. Tables listing the observed and calculated structure-factors and a .cif file may be obtained from the Depository of Unpublished Data, on the MAC website (document mammothite CM52 10.3749/canmin.1400048).

DESCRIPTION AND DISCUSSION OF THE STRUCTURE

Mammothite is a 'sparsely linked framework' structure (Eby & Hawthorne 1993). Figure 1 shows the octahedral layers of $[CuØ_6]$ and $[AlO_6]$ polyhedra cross linked by $[SbO_6]$ octahedra and $[PbØ_9]$ polyhedra. The sulfate tetrahedra are located in [010] tunnels and are bonded to the $[PbØ_9]$ polyhedra. Because of the passive role of the sulfate group, mammothite should not be considered in the sulfate chemical class, but in the oxide-hydroxide chemical class.

Coordination polyhedra around the atoms Pb, Cu, Al, Sb, and S

Mammothite has several interesting polyhedra in the crystal structure. The three Pb^{2+} sites have nine-fold coordination with two differing configurations: $[Pb1O_8Cl_1]$ mono-capped square antiprism polyhedron with face symbol $[3^{12}4^1]$ (Fig. 2a), while $[Pb21O_7Cl_2]$

TABLE 3. MAMMOTHITE: SELECTED BOND LENGTHS (Å) AND ANGLES (°)

Pb1–Oh52	2.599(2)	Pb21–O	2.383(4)	Pb22–O	2.367(4)		
Pb1–Oh51	2.606(2)	Pb21–Oh2	2.473(4)	Pb22–Oh2	2.462(4)		
Pb1–Os31	2.670(2)	Pb21–Os1	2.623(4)	Pb22–Os1	2.601(4)		
Pb1–Os32	2.624(3)	Pb21–Oh42	2.613(2)	Pb22–Oh41	2.639(2)		
Pb1–Oh32	2.671(2)	Pb21–Oh32	2.778(2)	Pb22–Oh31	2.805(2)		
Pb1–Os1	2.672(2)	Pb21–Os2	2.956(4)	Pb22–Os2	2.969(4)		
Pb1–Oh31	2.687(2)	Pb21–Cl2	3.087(1)	Pb22–Cl2	3.091(1)		
Pb1–Cl1	3.050(1)	Pb21–Os32	3.206(3)	Pb22–Os31	3.157(2)		
Pb1–Os2	3.066(2)	Pb21–Cl1	3.369(2)	Pb22–Cl1	3.370(2)		
<Pb1–Φ>	<2.738>	<Pb21–Φ>	<2.832>	<Pb22–Φ>	<2.829>		
Cu1–Oh52	1.927(2)	Cl1–Cl1	179.94(7)	Cu2–Oh52	1.948(2)	O–Oh1	169.19(5)
Cu1–Oh51	1.930(2)	Oh1–Oh52	94.11(9)	Cu2–Oh51	1.950(2)	Oh52–Oh51	87.21(8)
Cu1–Oh1	1.990(5)	Oh1–Oh51	86.22(8)	Cu2–Oh41	1.976(2)	Oh52–Oh42	96.7(1)
Cu1–Oh1'	2.007(5)	Oh1–Oh52	85.86(9)	Cu2–Oh42	1.983(2)	Oh41–Oh42	80.18(8)
Cu1–Cl1	3.406(2)	Oh1–Oh51	93.82(8)	Cu2–O	2.386(1)	Oh41–Oh51	95.5(1)
Cu1–Cl1'	3.415(2)			Cu2–Oh1	2.621(1)		
<Cu1–O>	<1.964>eq			<Cu2–O>eq	<1.964>		
<Cu1–Cl>	<3.410>ap			<Cu2–O>ap	<2.504>		
Al–Oh42 ×2	1.896(3)	Oh2–Oh2'	179.3(3)	Sb–O ×2	1.962(1)	O–O'	179.4(3)
Al–Oh2 ×2	1.910(1)	Oh41–Oh42	83.67(8)	Sb–Oh3 ×2	1.979(1)	Oh31–Oh31'	94.1(1)
Al–Oh41 ×2	1.927(3)	Oh42–Oh42'	96.7(2)	Sb–Oh32 ×2	1.997(2)	Oh31–Oh32	85.33(7)
<Al–O>	<1.911>			<Sb–O>	<1.979>		
S–Os32	1.445(3)	Os32–Os2	112.7(2)				
S–Os2	1.457(1)	Os32–Os31	108.6(1)				
S–Os31	1.474(3)	Os32–Os1	108.4(2)				
S–Os1	1.514(2)	Os31–Os2	113.1(2)				
<S–O>	<1.472>	Os1–Os2	107.8(1)				
		Os1–Os31	106.0(2)				

Φ denotes an O^{2-} or Cl^- anion.

D–H	D(D–H)	D(H...A)	<DHA>	D(D...A)	A
Oh1–H1	0.969	2.254	171.9	3.216	Os32
Oh2–H2	0.962	2.426	129.0	3.123	Os31
Oh31–H31	0.971	2.197	156.0	3.110	Cl2
Oh32–H32	0.969	2.199	160.9	3.132	Cl2
Oh41–H41	0.965	2.330	154.4	3.228	Cl1
Oh42–H42	0.965	2.311	168.2	3.262	Cl1
Oh51–H51	0.976	2.248	173.6	3.220	Cl2
Oh52–H52	0.971	2.494	132.2	3.227	Cl2

and [Pb22O$_7$Cl$_2$] are tri-capped trigonal prisms with face symbol [3^{14}] (Fig. 2b). These two configurations contrast in displaying the stereochemical active lone pair of electrons of the Pb^{2+} ion. The Cl atom in the [Pb1Ø$_9$] polyhedron is at the site one would expect for the lone pair electrons (Fig. 2c), while in the [Pb21Ø$_9$] and [Pb22Ø$_9$] polyhedra there are two Cl atoms that are spread apart, accommodating the lone pair (Fig. 2d). Also evident in the [Pb21Ø$_9$] and [Pb22Ø$_9$] polyhedra is a small deviation from the centric crystal system; H3, which is bonded to O3, falls off the mirror plane of the centric system, destroying its centric symmetry.

Both Cu^{2+} sites have distorted [4 + 2] octahedral coordination due to the Jahn-Teller effect. In the [Cu1O$_4$Cl$_2$] polyhedron (Fig. 3a), the distortion is very marked, with the average <Cu1–O> distance of 1.964 Å and the <Cu1–Cl> average of 3.411 Å compared to the [Cu2O$_6$] polyhedron (Fig. 3b) <Cu2–O$_{equitorial}$> distance of 1.964 Å and the <Cu2–O$_{apical}$> average of 2.503 Å. In the centrosymmetric structure both Cu sites are on special positions. Although both Cu sites in the acentric cell remain within one standard deviation of the 'special positions' of the centric cell, it is the H positions that destroy the inversion center of symmetry for [Cu1Ø$_6$] polyhedron (Fig. 3c) and also destroys the m-plane for [Cu2O$_6$] polyhedron (Fig. 3d). The Al and Sb sites are in regular octahedral coordination with mean bond lengths of <Al–O> 1.911 Å and <Sb–O> 1.980 Å. The average <Al–OH> bond
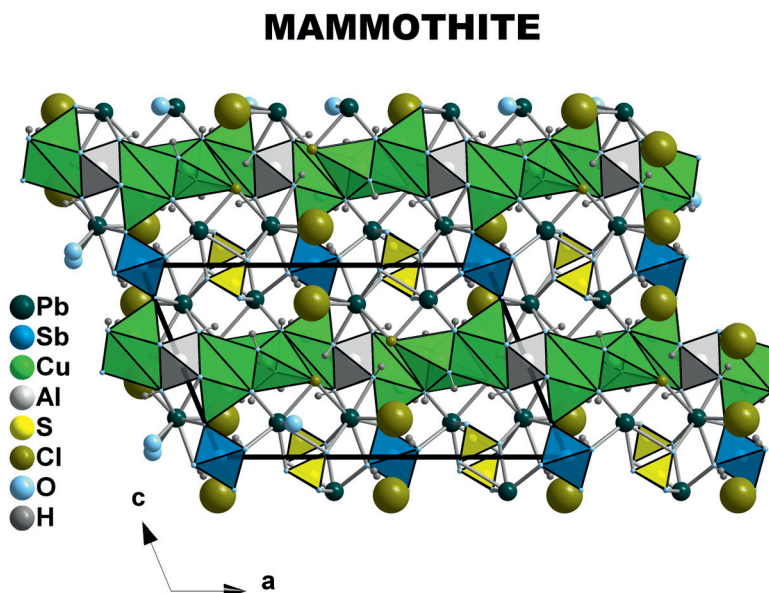
MAMMOTHITE

FIG. 1. Mammothite layered structure cross-linked into an open framework structure with [PbØ$_9$] polyhedra and sulphate groups in the cross-linking layer.
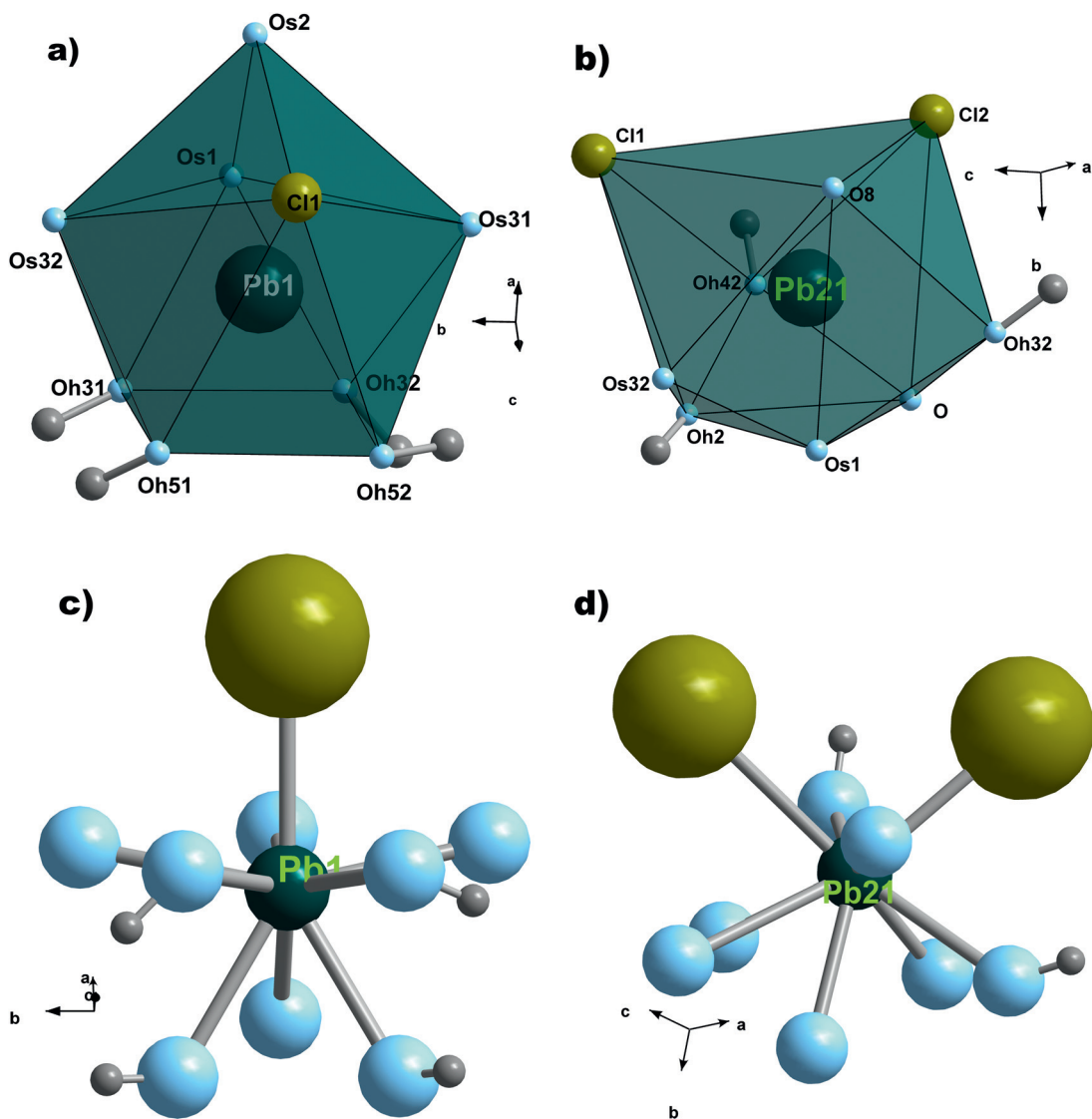
FIG. 2.   Coordination of Pb1 and Pb21 atoms. Note that the Pb22 atom coordination is almost identical to that of the Pb21 atom coordination. [Pb1O$_8$Cl$_1$] is a mono-capped square antiprism polyhedron while [Pb21O$_7$Cl$_2$] and [Pb22O$_7$Cl$_2$] are tri-capped trigonal prisms. Lead is nine-fold coordinated in all polyhedra. The [Pb21Ø$_9$] and [Pb22Ø$_9$] polyhedra display a coordination configuration typical of stereochemical lone-pair electrons.

distance, 1.911 Å, is larger than the ideal 1.885 Å, due to the addition of Cr, $^{[6]}$Cr^{3+} = 0.615 *versus* $^{[6]}$Al = 0.535 (Shannon 1976). The refined site-scattering is consistent with a site composition of Al$_{0.740}$Cr$_{0.260}$. Individual Al–O and Sb–O distances depart significantly from each other in *C*2 relative to Effenberger's *C*2/*m* as a result of different underlying octahedral site-symmetry.

The [SO$_4$] tetrahedron is quite distorted, with S–O bond lengths varying from 1.45 to 1.52 Å and subtended O–S–O angles varying from 106 to 113° (Table 3). The two H-bonds to O91 and O92 (Fig. 4) again violate the *m*-plane of symmetry in space group *C*2/*m*. The "slight torsion" of the [SO$_4$] group was well noted by Effenberger (1985), who attributed it to a possible "lowering of symmetry".
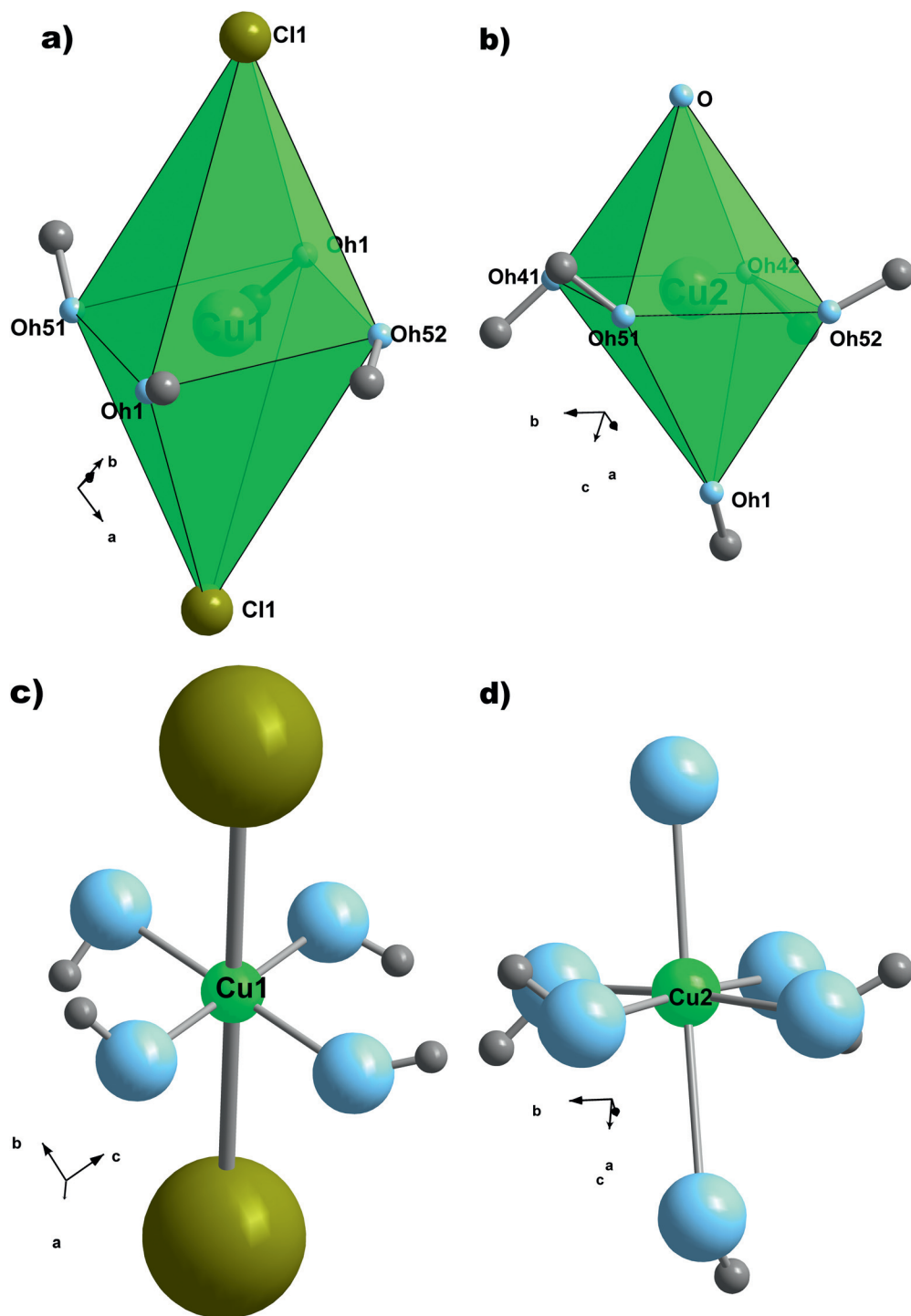
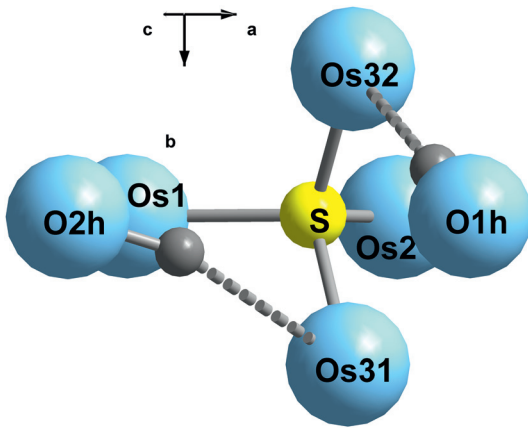FIG. 3. Coordination of the Cu1 and Cu2 atoms. Note that both [CuØ6] polyhedra display a Jahn-Teller effect.

FIG. 4. The [SO$_4$] tetrahedron showing H-bonds to the atoms Os31 and Os32 that torques the group into a distorted tetrahedron.

Octahedral and cross-linked layers

There are two distinct layers in the mammothite structure that parallel (001). There are three octahedral sites, two Cu and one Al, in the octahedral layer (Fig. 5). The [CuØ$_6$] octahedra form 'olivine-like' chains parallel to the **b**-axis. Because of the octahedral distortion, the chains are zigzagged, whereas the chain of [MgO$_6$] octahedra in olivine is straight. Euchroite has a similar [CuO$_6$] polyhedral chain, but one-half of the polyhedra are a regular octahedron, and the others are tetragonal dipyramids with one very long bond length, 2.80 Å (Fig. 6) (Eby & Hawthorne 1989). The chains in mammothite are cross-linked by edge-sharing [AlO$_6$] octahedra, leaving I-beam-shaped holes.

The second layer, termed the cross-linked layer, has three crystallographically distinct [PbØ$_9$] polyhedra that share edges, forming chains parallel to the **b**-axis, like the [CuØ$_6$] polyhedra (Fig. 7). The [Pb1Ø$_9$] polyhedron shares two edges with other [Pb1Ø$_9$] polyhedra (one with each [Pb211Ø$_9$] and [Pb221Ø$_9$] polyhedron) while the [Pb211Ø$_9$] and [Pb221Ø$_9$] polyhedra share a common edge, alternating along the chain. These chains are cross-linked by edge-sharing [SbO$_6$] octahedra and decorated with [SO$_4$] groups. These [SO$_4$] groups edge-share with each of the three Pb polyhedra but are not an important feature of the structure and hence don't warrant
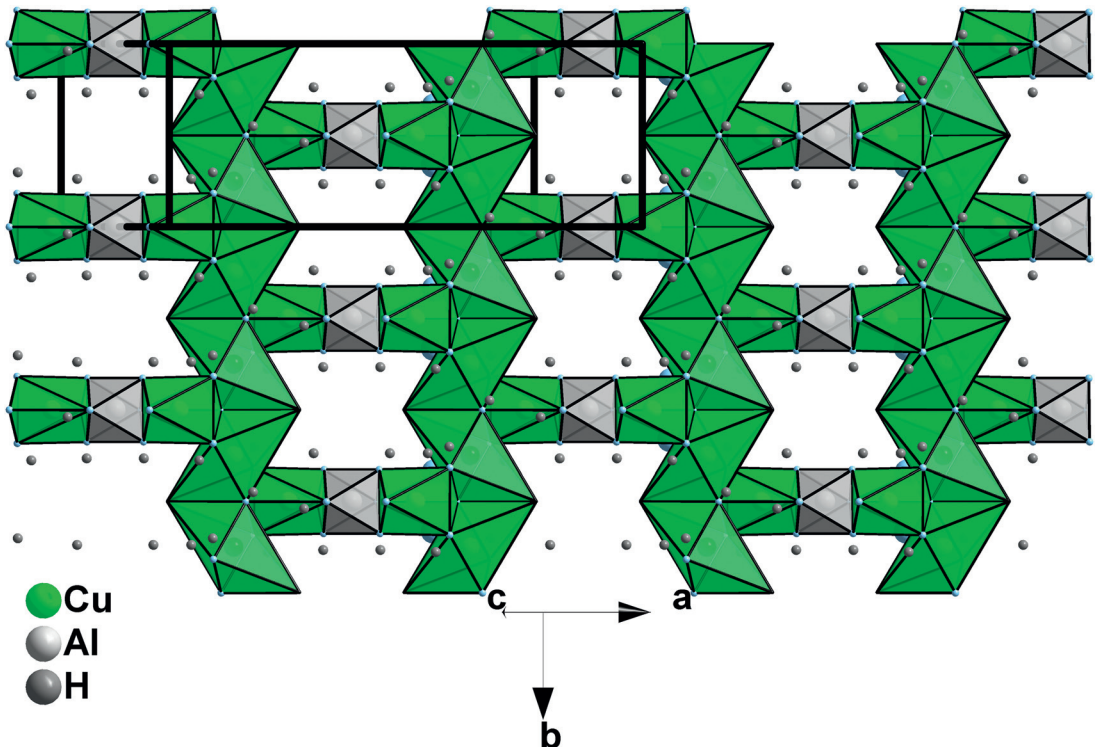

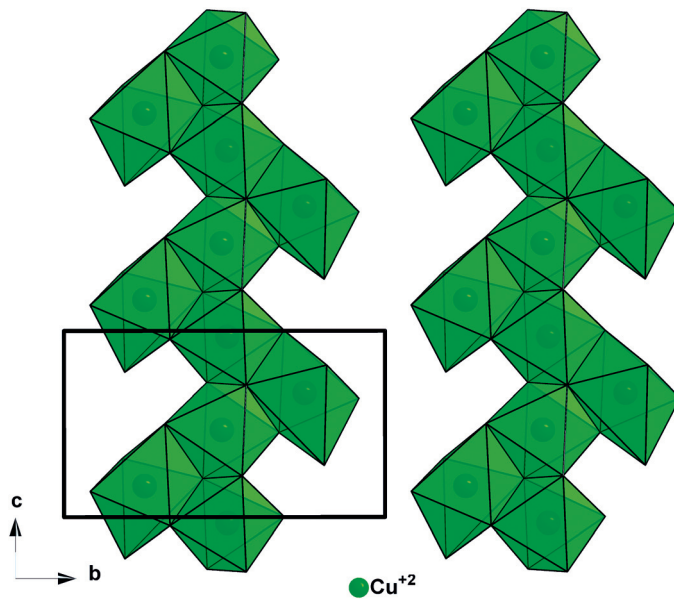FIG. 5. Mammothite (001) octahedral layer.

EUCHROITE
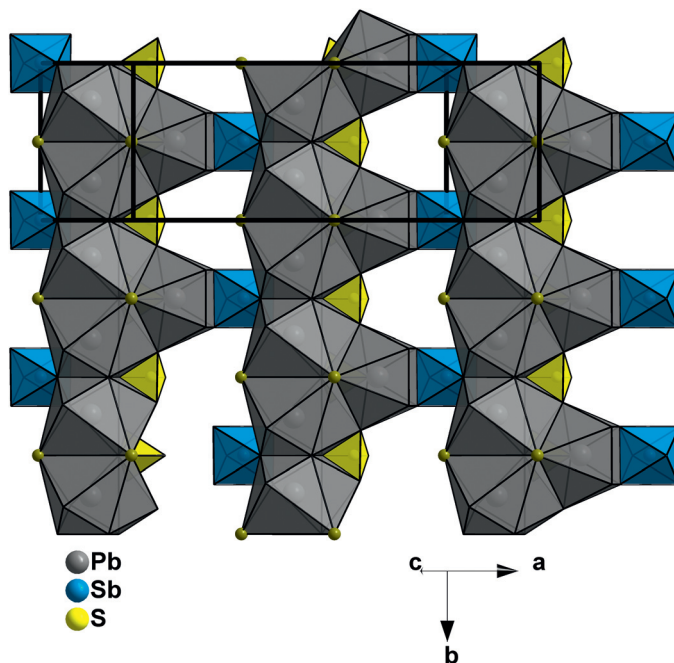

FIG. 6.   Euchroite octahedral chain.
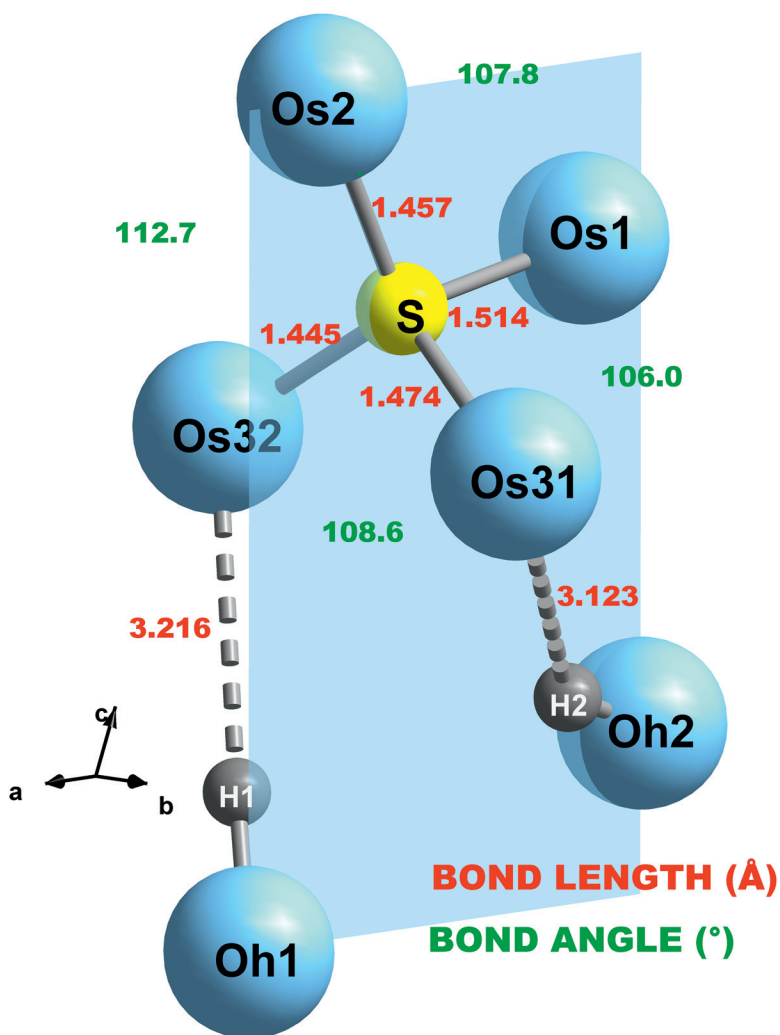

FIG. 7.   Mammothite (001) cross-linking layer.

FIG. 8.   The [SO$_4$] tetrahedron showing H-bonds to Os31 and Os32 that torques the group into a distorted tetrahedron. The blue shaded plane is (010), which is the *m*-plane in space group *C*2/*m*.

mammothite being classified as a sulfate. In this layer of polyhedra there are wedge-shaped holes. These holes do not align with the holes in the octahedral layer and they are not voids, as they are the site of the H atoms. The two layers are strongly bonded to each other, giving an open framework structure.

Looking at each layer helps to understand the reduction in symmetry from space group *C*2/*m* to *C*2. The octahedral layer (Fig. 5) has the *m*-plane. For the most part, even in the H positions, the octahedral layer is centrosymmetric. The cross-linking layer also has mirror symmetry when only the Pb, Sb, and S polyhedra are considered (Fig. 7). When the H positions are studied the symmetry breaks down and there is no more *m*-plane.

In the mammothite crystal structure presented by Effenberger (1985) in space group *C*2/*m*, oxygen atom Os3 in the sulfate-tetrahedral polyhedron is on a special position on the *m*-plane. This atom position, Os3, has two possible acceptor atoms from H atoms in hydroxyl groups Oh1 and Oh2. This gives two sets of "bifurcated hydrogen bonds". This, coupled with the "slight torsion of the [SO$_4$] group", led Effenberger to propose the possibility of a lower space group symmetry. In Figure 8 (a reorientation of Fig. 4) we see that space group *C*2 satisfies these criteria. The Os3 ^ Os3 angle 109.8° of Effenberger (1985) is no longer near the ideal tetrahedral angle of 109.5°, but is considerably smaller for Os31 ^ Os32 = 108.6(1)°. In addition, the S–O bond lengths are no longer equal (1.445(3) and 1.474(l) Å).

CONCLUSIONS

Mammothite provides an example of a crystal structure solution that is now possible due to improvements of equipment and data handling. Prior to this time the determination of H positions would not be possible in a mineral having such a concentration of Pb atoms, due to absorption corrections. Higher X-ray beam intensity and more sensitive detectors reduce this problem to a manageable degree. The crystal structure refinement based on the increased accuracy in the data show features that were not detectable in former times. It may be that many problems occurring in older descriptions of minerals could now be refined, giving an improved understanding of the crystal chemistry of hydrogen bonding and its ramifications.

REFERENCES

BRESE, N.E. & O'KEEFFE, M. (1991) Bond-valence parameters for solids. *Acta Crystallographica* **B47**, 192–197.

EBY, R.K. & HAWTHORNE, F.C. (1989) Euchroite, a heteropolyhedral framework structure. *Acta Crystallographica* **C45**, 1479–1482.

EBY, R.K. & HAWTHORNE. F.C. (1993) Structural relationships in copper oxysalt minerals. I. Structural hierarchy. *Acta Crystallographica* **B49**, 28–56.

EFFENBERGER, H. (1985) The crystal structure of mammothite, $Pb_6Cu_4AlSbO_2(OH)_{16}Cl_4(SO_4)_2$. *Tschermaks Mineralogische und Petrographische Mitteilungen* **34**, 279–288.

IBERS, J.A. & HAMILTON, W.C., EDS. (1974) *International Tables for X-ray Crystallography IV*. The Kynoch Press, Birmingham, United Kingdom.

KIRKEMO, H., ANDERSON, C.A., & CREASEY, S.C. (1965) Investigations of molybdenum deposits in the conterminous United States 1942–1960. *Contributions to Economic Geology, United States Geological Survey Bulletin* **1182-E**, 6–9.

MALCHEREK, T. & SCHLÜTER, J. (2007) $Cu_3MgCl_2(OH)_6$ and the bond-valence parameters of the OH–Cl bond. *Acta Crystallographica* **B63**, 157–160.

PEACOR, D.R., DUNN, P.J., SCHNORRER-KÖHLER, G., & BIDEAUX, R.A. (1985) Mammothite, a new mineral from Tiger, Arizona, and Laurium, Greece. *Mineralogical Record* **16**, 117–120.

SHANNON, R.D. (1976) Revised effective ionic radii and systematic studies of interatomic distance in halides and chalcogenides. *Acta Crystallographica* **A32**, 751–767.

SHELDRICK, G.M. (1997) *SHELX-97 Program for the Solution and Refinement of Crystal Structures*. Siemens energy and Automation, Madison, Wisconsin, United States.

SHELDRICK, G.M. (1998) *SADABS User Guide*. University of Göttingen, Göttingen, Germany.

STEWART, L.A. & PFISTER, A.J. (1960) Barite deposits of Arizona. *U.S. Bureau of Mines Report of Investigation* **5651**, 41–44.